Strojniški vestnik - Journal of Mechanical Engineering 69(2023)5-6, 235-247
DOI:10.5545/sv-jme.2023.558
Original Scientific Paper
Received for review: 2023-02-27
Received revised form: 2023-04-12
Accepted for publication: 2023-04-14

Experimental Study and Numerical Analysis on Windage Power Loss Characteristics of Aviation Spiral Bevel Gear with Oil Injection Lubrication

Linlin Li — Sanmin Wang
Northwestern Polytechnical University, School of Mechanical Engineering, China

With the increasing speed of aviation spiral bevel gears, the load-independent windage power losses caused by hydrodynamic have increasingly more influence on gear transmission efficiency. Firstly, a test rig for the windage power loss of spiral bevel gear under oil-jet lubrication is established, and on this basis, a method for measuring windage torque is proposed. Next, the interactive effects of different injection lubrication parameters on the windage power loss were studied by orthogonal experiment, and the formula for calculating the windage loss was obtained by fitting the experimental data. Then, the fluid distribution, velocity field and pressure field around the gear were analysed by using a computational fluid dynamics (CFD) numerical model, and the mechanical and energy characteristics of the gear windage power loss were obtained. Finally, the dimensionless processing of the windage moment was carried out, and the variation of the dimensionless windage moment coefficient with the rotational Reynolds number is obtained. The comparison between the dimensionless windage moment coefficient of experimental data and simulation results shows that the CFD values are in good agreement with the measured data. This study provides experimental and methodological guidance for the calculation of windage power loss and windage reduction design of aviation gear pair under oil injection lubrication.

Key words: spiral bevel gear, oil-jet lubrication, windage power loss, windage test

Highlights

- *A test rig for the windage power loss of spiral bevel gears under oil-jet lubrication is established.*
- *A method for measuring windage torque is proposed.*
- *The interactive effects of different injection lubrication parameters on the windage power loss were studied with orthogonal experimentation.*
- *The comparison between the dimensionless windage moment coefficient of experimental data and simulation results shows that the CFD values are in good agreement with the measured data.*

0 INTRODUCTION

Aviation spiral bevel gears mainly work at high speed and high power. Therefore, the oil injection mode is mostly used to provide lubricating oil to the gear system [1]. When the fluid impacts the gear teeth, the two tooth surfaces in a tooth space are respectively represented as a suction surface and a pressure surface. The pressure differential force will produce a torque opposite to the rotation direction of gears; at the same time, the viscous force between the fluid and the gear surface will also cause the reverse torque. These two torques constitute the windage torque of the gear, thus resulting in windage power loss [2], which is a load-independent power loss. A large number of experiments show that the windage loss becomes significant with the increase of gear speed [3]. When the linear velocity of the gear is greater than 50 m/s, the windage power loss caused by hydrodynamic behaviour must be paid sufficient attention [4] to [6]. Handschuh [7] pointed out that when the linear velocity of the gear reaches 125 m/s, the windage loss of the gearbox accounts for about half of the load-independent power loss and can dominate other loss mechanisms. At the same time, the windage effect will deflect the trajectory of lubricating oil flow, making it difficult for lubricating oil to enter the gear meshing area. This causes dry friction of the gear, and subsequent tooth surface scuffing, wear, etc. Furthermore, the additional heat generated by the windage power losses can easily aggravate the temperature rise of the gear [8] and [9].

The main methods to study the windage power loss of gearboxes are theoretical analysis, experimental measurement, and numerical simulation [10]. Physical experiments were mainly used in early literature research. Computational fluid dynamics (CFD) provides help for the visual analysis of gear windage losses and provides the possibility for the study of some complex phenomena that cannot be realized under conventional experimental conditions [11] and [12]. Researchers, such as Anderson and Loewenthal [13], Dawson [14] and Diab et al. [15], mainly used experimental methods to study the windage power loss of a single spur gear in a single-phase air flow. Considering the influence of gear

*Corr. Author's Address: Northwestern Polytechnical University, School of Mechanical Engineering, China, hnlilinlin@126.com

geometric parameters, working conditions, fluid properties and other factors on the windage loss, some empirical formulas for calculating the windage loss of spur and helical gears are obtained according to the experimental results. Finally, some methods to reduce windage power loss are proposed. Winfree [16] obtained a large number of experimental data on the windage loss of spiral bevel gears. The results show that the shroud can greatly reduce the windage power loss of high-speed spiral bevel gears, and a series of design principles for a gear system to reduce the windage power loss are proposed. Seetharaman and Kahraman [17] established a simplified computational fluid dynamics model to study the windage power loss of meshing spur gears to explain the suction/extrusion effect of gear meshing on windage loss. The model showed that the squeezing power loss in the meshing area contributed the most to the total windage loss. Ruzek et al. [18] used an improved test rig to study the windage power loss of disk, spur, and helical gears under various combinations through a series of experiments. Their results show that although there is coupling interaction when the two gears are engaged, the windage loss of the gear pair is about equal to the sum of the individual windage loss values when the two gears are not engaged. These findings are also verified by the sliding grid method and multi-reference rotation (MRF). Delgado and Hurrell [19] and Handschuh and Hurrell [20] performed experiments at the Glenn Research Center of NASA, US and obtained a large number of windage loss data of spur gears under different experimental conditions. The influence factors of windage power loss are studied from the aspects of gear geometry, shroud shape, different lubrication system configuration, pressure, temperature and meshing effect, and an empirical model for calculating the windage power loss of spur gears is formed.

Massini et al. [21] experimentally measured the parameters related to the windage loss of a single spur gear under free lubrication; they used particle image velocimetry (PIV) technology to measure the velocity and vector diagram of flowing fluid. This is the first experimental work to realize the visualization of flow fields near high-speed gears with PIV technology. Maccioni et al. [22] established a CFD model capable of taking aeration into consideration and developed a new solver. A dip-lubricated tapered-roller-bearing was simulated with the new solver and a standard one. The numerical predictions were compared with the experimental data obtained on a dedicated test rig using PIV. The results show that the numerical values in all rotation ranges are in good agreement with the experimental results. Mastrone and Concli [23] presented a new mesh handling strategy specifically suited to studying the efficiency and lubrication inside gearboxes transmissions. The methodology is based on the Global Remeshing Approach with Mesh Clustering (GRA^{MC}) process that drastically reduces the simulation time by minimizing the effort for updating the grids. Compared with the power loss measured via experimentation, the proposed method has good accuracy. Gorla et al. [24] systematically studied the effects of lubricating oil density, viscosity, gear circumferential velocity, addendum circle diameter, tooth width and other factors on the hydraulic loss of a gearbox system by CFD and carried out experimental verification. Fondelli et al. [25] used volume of fluid (VOF) model to simulate and analyse a single spur gear and adopted a mesh adaptive method to simulate the process of lubricating oil jet impacting on the tooth surface of a single high-speed gear so as to estimate the resistance moment of the lubricating oil jet and analysed the influence of the injection angle on the resistance moment and lubrication performance, thereby improving the gear transmission efficiency and saving the cost of simulation experiments. Farall et al. [26], Rapley et al. [27] and Webb et al. [28] mainly analysed the windage loss of a single spiral bevel gear in single-phase air flow by CFD. The characteristics of an air flow field around gears with and without shroud are analysed from several angles, and the influence of different configurations of the shroud on the fluid distribution around gears is analysed, which provides guidance for the optimal design to reduce windage loss. Johnson et al. [29] and Simmons et al. [30], on the basis of previous studies, used the windage test bench of the gas turbine transmission centre of Nottingham University, UK to obtain the variation law of windage power loss of a single spiral bevel gear and gear pair under different shrouds, gear rotation directions, lubrication conditions, and other parameters. Subsequently, the pressure and lubrication system are added to the bench, so that the experimental platform can form a high-pressure environment and oil mist in the gear box. The results show that the lubrication condition increases the density of fluid around the gear and Reynolds number. For gears unshrouded, the existence of lubricating oil increases the windage moment; however, the windage loss does not change much for the gear shrouded.

According to the analysis of the existing literature, there is little research on the windage power loss caused by the flow field around the spiral bevel gear pair and the two-phase flow of oil injection

lubrication, especially the theoretical analysis and experimental research on the influence of oil injection lubrication parameters on the windage loss of spiral bevel gear pair. In this paper, a test bench for measuring the windage power loss of spiral bevel gears during oil injection lubrication is established. The method for measuring the windage loss of gear pairs is proposed, and the interactive effects of different oil injection parameters on gear windage losses are obtained with orthogonal experiments. Then, based on the tooth surface movement method, the oil injection lubrication model of spiral bevel gear is established. The instantaneous distribution of two-phase fluid and the changes law of the pressure field and velocity field in the gearbox are simulated and analysed by using the Fluent software and the dynamic mesh technology. The mechanical and energy characteristics of windage losses of spiral bevel gears with oil injection lubrication are obtained, which provides a theoretical reference for the calculation of windage and windage reduction design of aviation spiral bevel gears.

1 EXPERIMENTAL SETUP AND MEASUREMENT

1.1 Test Rig

The windage power loss test experiment of spiral bevel gears adopts an open power flow gear test device, as shown in Fig. 1. The experimental equipment mainly includes a high-speed spindle, low-speed shaft, flexible coupling, bearing, variable frequency speed regulating motor, torque-speed sensor, temperature sensor, pressure sensor, eddy current brake, oil injection lubrication circuit system, and signal acquisition and processing system.

As shown in Fig. 1, the motor can rotate in both directions, and the maximum speed of the drive gear shaft can reach 10,000 rpm. The non-contact strain gauge torque sensor can measure the forward and reverse torque without zero adjustment and commutation and is not limited by the speed. At the same time, several pulse counters are integrated into the sensor, and the speed of the gear shaft can be output by calculating the number of pulses output by the photoelectric encoder. The accuracy of this sensor is ≤ 0.2 % full scale, and the sensitivity drift is 0.009 % per °C in the temperature range of 0°C to 50 °C.

The signal acquisition and processing system is used to collect and process all the measurement data, including shaft speed, torque, inlet and outlet oil temperature and oil pressure, as shown in Fig. 2.

The speed of the rotating shaft is set by the motor and controlled by the speed adjustment knob on the operation panel. The speed value is measured by the speed sensor and displayed on the panel. The inlet and outlet oil temperatures are measured by the temperature sensor of the oil injection lubrication system. Meanwhile, the windage torque of the gear and the friction torque on the bearing and the rotating shaft are measured by the torque sensor and also recorded on the instrument panel.

Lubrication of gears and bearings is provided by a special oil control system, as shown in Fig. 3. This system can provide lubricating oil with controlled oil temperature and oil pressure. The vacuum oil pump is connected to the pipeline system and the gate valve to adjust the oil supply pressure continuously within the range of 0 MPa to 1 MPa. The oil heater can adjust the oil temperature at any time and monitor the change

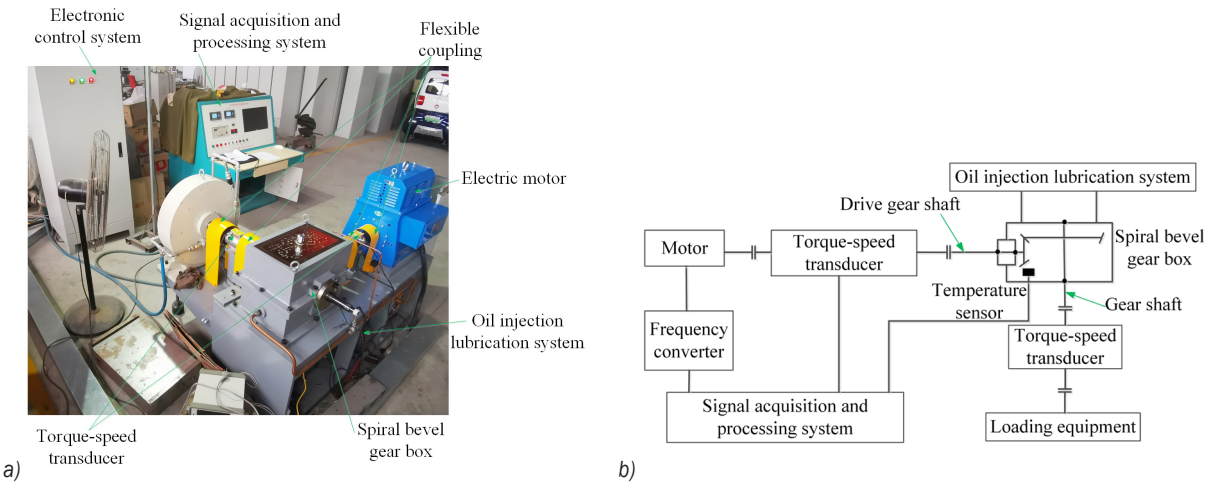

Fig. 1. *a) View of the test rig, and b) schematic representation of test rig*

of oil temperature through the thermometer on the oil tank.

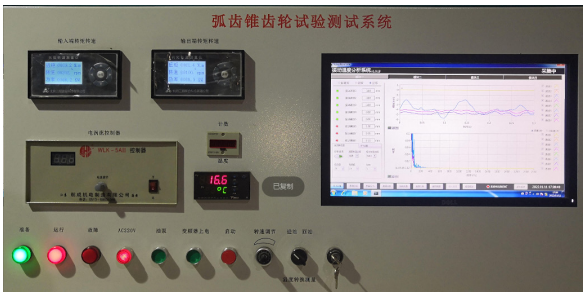

Fig. 2. *Signal acquisition interface*

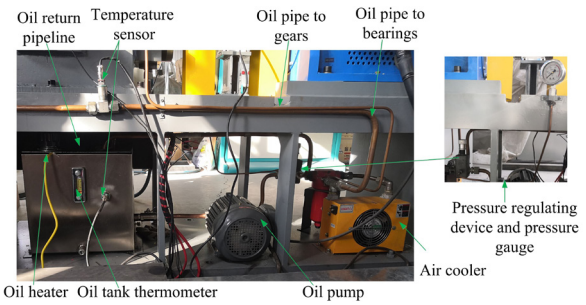

Fig. 3. *Oil injection lubrication system*

1.2 Experimental Measurement Scheme

At present, according to most documents on gear windage experiments [21], [29] and [30], the method to measure the rig driveline torque of rotating shafts and bearings is to measure the system torque with the gear pair removed and take this measurement value as the extra power loss caused by shafts and bearings in the gear transmission system. According to Ruzek et al. [18], gear pairs do not significantly change the additional power loss generated by bearings and rotating shafts. This is because, based on the Harris equations [31], it is found that the addition of the gear pair produces an additional power loss of less than 1 W in the entire speed range. Consequently, the effect of the gears on the rig driveline torque is considered negligible. Therefore, in this experiment, when the gear pair rotates at a low speed (input shaft speed ≤ 1000 rpm) and without load, the torque value measured when it is small and changes little with the increase of speed is taken as the rig driveline torque generated by the friction of the bearing, the rotating shaft, and the engagement of the gear pair without load. This is because the windage loss of the gear is small and can be ignored. At the same time, this method can eliminate the influence of the extra power loss caused by the no-load meshing of the gear pair on the experimental measurement of the windage loss. Therefore, the windage torque of the experimental gear is the value obtained by subtracting the rig driveline torque from the measured value of the torque sensor when the system is unloaded.

When measuring the windage torque of a gear under oil injection lubrication, the friction torque of the rotating shaft, bearing and gear pair without load will change with the differences in injection temperature, injection pressure, and rotating shaft speed. According to the experimental research of Massini [21], the influence relationship is as follows:

$$M_f = a \cdot u_p^b \cdot T^c \cdot P^d, \tag{1}$$

where, M_f is the rig driveline friction moment; a, b, c, d are the fitting coefficients of experimental data; u_p is the pitch circular linear speed of the rotating gear; T and P are injection temperature and pressure, respectively.

Therefore, according to different gear working conditions and oil injection lubrication conditions, the rig driveline torque in the measurement of windage loss needs to be corrected according to Eq. (1).

1.3 Measurement and Calculation of Windage Power Loss

The geometric parameters of experimental spiral bevel gears are shown in Table 1.

Table 1. *Basic parameters of spiral bevel gear*

Parameters	Pinion	Gear
Number of teeth	27	81
Heel module [mm]	3.85	
Pressure angle [°]	20	
Helix angle [°]	35	
Outer cone distance [mm]	164.31	
Tooth width [mm]	49	
Outside tip diameter [mm]	112.72	313.07
Rotation direction	Left	Right

The gear pair is lubricated by oil injection at the into-meshing side and out-of-meshing side at the same time. The diameter of the oil nozzle is 4 mm. According to the basic parameters of spiral bevel gears in Table 1, the tested gear pair is shown in Fig. 4.

In order to reduce the dispersion of measurement results during the test, for each test condition, run at a constant speed for ten minutes before measuring power loss. The test was repeated five times under each operating condition, and the average value was taken as the measurement value. Fig. 5 shows the

scatter plot of the average value and standard deviation of the gear windage power curve at different speeds.

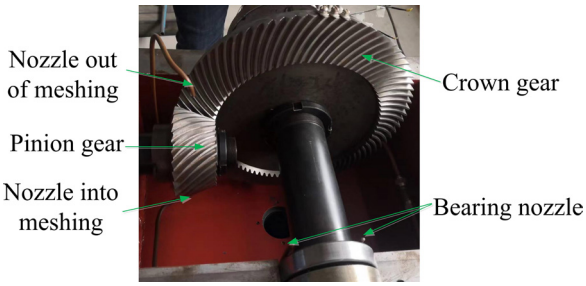

Fig. 4. *Gear pair and lubrication*

It can be seen from Fig. 5 that the standard deviation of the measured torque is about 2.3 % to 3.1 % of its average value, which indicates that the dispersion degree of each set of measurement data is not significant, so the repeatability of the test measurement is good.

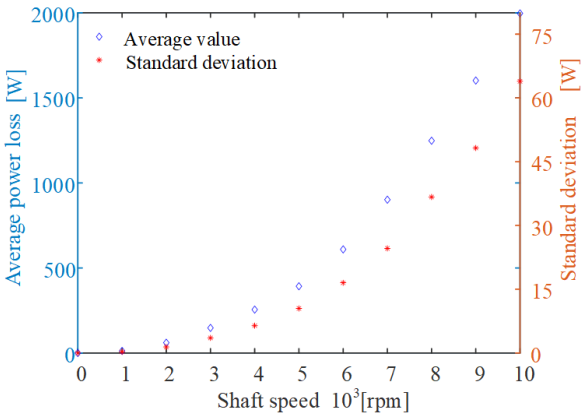

Fig. 5. *Average value and standard deviation of power loss value measured by experiment*

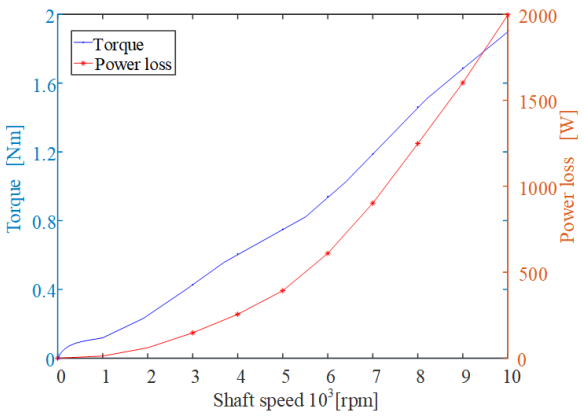

Fig. 6. *Torque value and power loss value measured experimentally with different speeds*

The injection temperature is set at 20 °C, the injection pressure is at 0.2 MPa, and the brake is unloaded. The motor speed button on the control panel is adjusted to continuously increase the speed from 0 rpm to 10,000 rpm. At the same time, the torque values at different speeds are recorded and the power loss values are calculated. The results are shown in Fig. 6.

As can be seen from Fig. 6, the power loss of the gear system is less than 10 W when the rotational speed is less than 800 rpm. According to the windage measurement scheme in Section 2.2, this experiment assumes that the power loss measured when the speed is lower than 800 rpm is the additional power loss caused by the friction of the gear shaft, bearing and gear pair engagement. At the same time, by changing different injection temperatures and pressures and correcting this torque according to Eq. (1), the windage torque and rig driveline torque values of the experimental gear pair at different rotational speeds are calculated, as shown in Fig. 7.

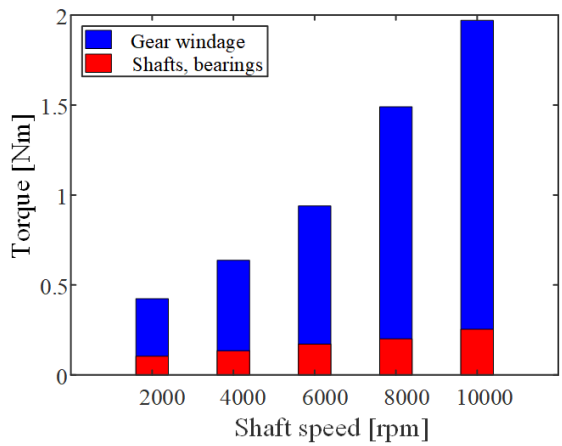

Fig. 7. *Distribution of windage torque and rig driveline torque at different rotating speed*

It can be seen from Fig. 7 that the windage torque of the gear pair increases sharply with the increase of the speed, but the rig driveline torque changes little with the speed. This indicates that the higher the rotational speed, the greater the proportion of the windage loss of the gear pair to the total load-independent power loss. This is because the friction force of the bearing, shaft and gear pair engagement without load is small, and the rotational speed has little effect on it. However, with the increase of the gear pair speed, the velocity of the flow field around the gear increases, and the rotating Reynolds number increases. At this time, the power consumed by gear

rotation is greater; that is, the reverse moment of fluid movement to gear rotation increases.

1.4 Interaction of Injection Parameters on Windage Loss

In addition to the rotational speed, the oil injection parameters are also important factors affecting the windage loss of gear pair under oil injection lubrication. Therefore, in order to seek the interaction law of injection parameters on gear windage loss, orthogonal tests are used to analyse the influence of these variables on the results. Orthogonal testing [32] can use relatively few representative data to analyse the influence of various factors on the test results. The test index of this test is the gear windage power loss calculated by subtracting the rig driveline torque from the measured torque. The shaft speed (A), oil injection pressure (B), and oil injection temperature (C) are the test factors. The level of each test factor is set as four, as shown in Table 2.

Table 2. *Factor level*

Levels	Factors		
	A Shaft speed [rpm]	B Oil-jet pressure [MPa]	C Oil-jet temperature [°C]
1	2000	0.1	20
2	4000	0.2	25
3	6000	0.3	30
4	8000	0.4	35

Table 3. *Experiment scheme and result*

Test numbers	Column (Factors)			Windage power loss [kW]
	A	B	C	
1	2000	0.1	20	0.063
2	2000	0.2	25	0.069
3	2000	0.3	30	0.075
4	2000	0.4	35	0.082
5	4000	0.1	25	0.176
6	4000	0.2	20	0.184
7	4000	0.3	35	0.197
8	4000	0.4	30	0.222
9	6000	0.1	30	0.421
10	6000	0.2	35	0.440
11	6000	0.3	20	0.478
12	6000	0.4	25	0.534
13	8000	0.1	35	1.030
14	8000	0.2	30	1.056
15	8000	0.3	25	1.123
16	8000	0.4	20	1.215

The standard orthogonal table $L_{16}(4^3)$ is selected to carry out the experimental analysis of 16 groups of factor combinations, and the windage power loss of each combination is obtained. The results are shown in Table 3.

The gear windage power loss of each factor at each level is added; then, its average value is calculated and recorded as $\overline{Y}_i$. Finally, the range of each factor was calculated and recorded as R_j. The range values are arranged in order, as shown in Table 4.

Table 4. *Analysis of variance*

Test	Column (Factors)		
	A	B	C
$\overline{Y}_1$	0.072	0.423	0.485
$\overline{Y}_2$	0.195	0.437	0.475
$\overline{Y}_3$	0.468	0.468	0.443
$\overline{Y}_4$	1.106	0.513	0.437
R_j	4.134	0.362	0.191
Influence order: A>B>C			

From the range in Table 4, it can be seen that the interaction degree of each factor on the test results is A, B and C in descending order, among which significant factors are A and B, and C is insignificant. That is, the shaft speed has the greatest influence on the windage power loss of the gear pair, followed by the injection pressure, and both are positively correlated. The less affected is the injection temperature; it is negatively correlated.

In order to further study the interactive influence of various factors on the test indicators, the experimental data in Table 4 are fitted with polynomial curves to obtain the calculation formula of the windage power loss of spiral bevel gear pairs with test factors as independent variables. Since the polynomial objective function in the form of a power function has the least generalization and residuals, the following power function is obtained:

$$P_w = 0.0436 \cdot N^{2.71} \cdot P^{0.10} \cdot T^{-0.07}, \quad (2)$$

where P_w is the windage power loss of gears; N is the shaft speed; P the oil injection pressure; T is the oil injection temperature.

According to Eq. (2), the windage power loss of the spiral bevel gear is approximately proportional to the 2.71 power of gear speed. The empirical formulas and experiments on gear windage power losses by Anderson and Loewenthal [13], Dawson [14] and Diab et al. [15] show that the windage power loss is approximately proportional to the third power of rotational speed, and it is also related to gear parameters, fluid medium parameters and boundary

conditions. This paper is consistent with the above research conclusions. This shows that rotational speed remains the most important factor affecting the windage power loss of gear under oil injection lubrication.

In this experiment, the injection quantity is changed by adjusting the injection pressure. When the diameter of the nozzle is constant, the injection pressure is proportional to the square of the flow rate. The larger the injection pressure, the more the injection flow rate, which leads to higher injection velocity. At this time, the lubricating oil sprayed from the nozzle has greater kinetic energy and momentum, and the ability to resist the influence of high-speed fluid around the gear is stronger so that the volume fraction of the lubricating oil on the tooth surface becomes larger. Therefore, with the increase of the injection velocity, more lubricating oil can enter the meshing area of the gear pair, thereby increasing the pumping power loss of the gear pair meshing interface.

The accuracy of the calculation of windage losses significantly influences the efficiency of the gear system. At present, in engineering applications, when calculating the efficiency of the spiral bevel gear system, the power loss values mainly refer to the recommended values of AGMA standards, ISO standards or national standards [33], and there is no specific calculation formula. Therefore, the fitting formula of windage power loss based on oil injection lubrication parameters provides a theoretical reference for the efficiency calculation of spiral bevel gears. At the same time, by analysing the interactive influence law of oil injection parameters on gear windage losses, it provides theoretical and methodological guidance for the next research on the method of reducing windage power loss.

2 NUMERICAL SIMULATION MODEL OF SPIRAL BEVEL GEARS

2.1 Basic Governing Equations of Flow Field

The governing equations of the mass and momentum conservation for the fluid domain inside the gearbox are given as [21]:

$$\frac{\partial \rho}{\partial t}+\nabla\cdot(\rho\mathbf{V})=0, \tag{3}$$

$$\frac{\partial(\rho\mathbf{V})}{\partial t}+\nabla\cdot(\rho\mathbf{V}\mathbf{V})= -\nabla p+\nabla\cdot\left[\mu\left(\nabla\mathbf{V}+\nabla\mathbf{V}^{T}\right)\right]+\rho\mathbf{g}+\mathbf{F}, \tag{4}$$

where ρ is the density. t is the time. $\mathbf{V}$ is the velocity vector. $\mathbf{g}$ is the gravity vector. $\mathbf{F}$ represents the external forces. μ is the viscosity. These basic equations should be applied to each cell.

The lubrication process of gear pair is a problem of oil-air two-phase flow, which needs to be analysed with multi-phase flow numerical calculation. Therefore, density and viscosity of the mixture are computed as

$$\rho=\alpha\rho_a+(1-\alpha)\rho_i,\quad \mu=\alpha\mu_a+(1-\alpha)\mu_i, \tag{5}$$

where, the subscripts a and i represent air and oil, respectively; α is the volume fraction of air, and it can be calculated for all cells as

$$\frac{\partial\alpha}{\partial t}+\frac{\partial(\alpha u_i)}{\partial x_i}=0. \tag{6}$$

2.2 CFD Model of Gear Pair

In order to accurately describe the hydrodynamic characteristics of the oil-gas two-phase flow in the spiral bevel gearbox. To avoid the interference of unnecessary parts in the box, a simplified geometric model of the spiral bevel gearbox was established using Unigraphics (UG) software, ignoring the web plate hole, bearings, flange structure, fixings, etc. The final three-dimensional model of the gearbox and the coordinate system are shown in Fig. 8.

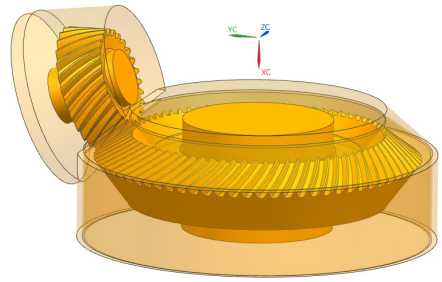

Fig. 8. *3D model of spiral bevel gearbox*

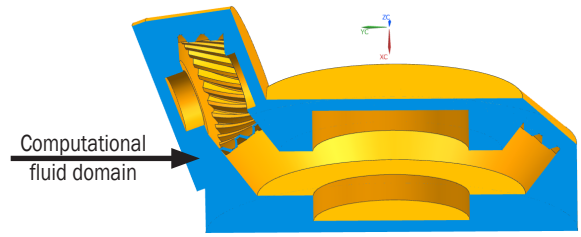

Fig. 9. *Computational domain flow field model*

It is necessary to calculate the interaction between the flow field and the gear with CFD simulation.

Therefore, when extracting the internal flow field of the gearbox, a closed boundary is adopted without considering the influence of the microstructure of the gearbox body. The computational fluid domain flow field model is obtained via a Boolean operation between the gearbox and the gear pair, as shown in Fig. 9.

The gearbox geometry model was imported into the pre-processing software ANSYS-ICEM CFD, and the fluid domain was discretized into unstructured tetrahedral meshes based on the finite volume method, to obtain the fluid dynamics analysis model. The mesh model of the gearbox is shown in Fig. 10.

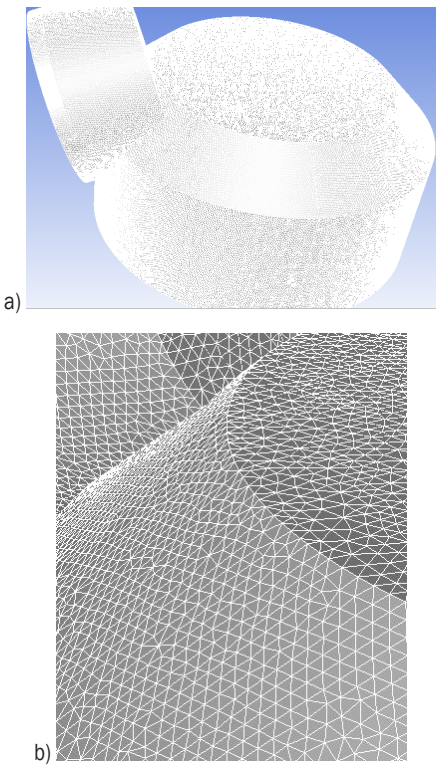

Fig. 10. *Mesh model of the gearbox; a) global view, and b) partial view*

To improve the precision and reliability of the simulation results, a mesh independence analysis is performed to ensure that discretization errors are quantified and minimized. This was done by comparing the windage moment at a rotating speed of 8000 rpm. The number of these meshes and the windage moment values measured are shown in Table 5.

As shown in Table 5, the windage moment can be considered stable when the number of mesh elements exceeds 1,626,730. In order to ensure the accuracy of CFD calculation, reduce calculation time and save calculation resources, it is necessary to densify and refine the mesh locally on each surface of the gear and near the oil injection nozzle. At the same time, in order to obtain high-quality mesh, it is necessary to smooth the mesh. The maximum mesh size of the fluid domain is 3 mm, the boundary layer size is 0.4 mm at tooth surface, end face and nozzle. Finally, the number of mesh elements in the entire fluid domain of the calculation model is about 1.65 million.

Table 5. *Results of mesh independence analysis*

Mesh	Total mesh elements	Windage moment [N·m]
1	357,162	2.95
2	621,376	2.13
3	916,405	1.26
4	1,457,573	1.50
5	1,626,730	1.46
6	1,912,642	1.43

2.3 CFD Methodology

The pre-processed model is imported into Fluent for solution. A CFD code that applies the VOF method to model free surface flow was utilized to simulate the two-phase flow. The boundary movement was defined through the UDF file, and the mesh update process was automatically completed by Fluent according to the change of the boundary in each iteration step. The solution settings are shown in Table 6.

Table 6. *Settings of numerical calculation*

Description	Parameter value
Equation control calculation method	Pressure-based separation solver
Time	Transient
Multiphase model	VOF model (implicit body force activated) Primary phase: air Secondary phase: oil
Viscous model	SST k–ω
Inlet boundary	Velocity-inlet
Outlet boundary	Pressure-outlet
Wall condition	Non-slip
Dynamic mesh	Smoothing and local Remeshing
Discretization schema	Pressure velocity coupling: PIMPLE Spatial discretization: Second order upwind
Initialization	Standard initialization

2.4 Formation Mechanism of Gear Windage Loss

The fluid velocity vector around the tooth is shown as Fig. 11, which shows that the direction of fluid flow is opposite to the direction of gear rotation.

As can be seen from Fig. 11, when the gear rotates, the fluid around it will be separated at the tooth top. Some of the fluid flows over the top of the tooth without changing its direction. Moreover, the other part is sucked into the gap between the teeth from the position close to the tooth top and forms eddy currents in the tooth space. The tooth surface impacted by fluid appears as the pressure surface as shown in Fig. 12a, with local high pressure; Then the leeward side is shown as the suction surface as shown in Fig. 12b, and local low pressure occurs, resulting in a pressure difference between the two tooth surfaces and a pressure difference torque, which is opposite to the rotation direction of the gear.

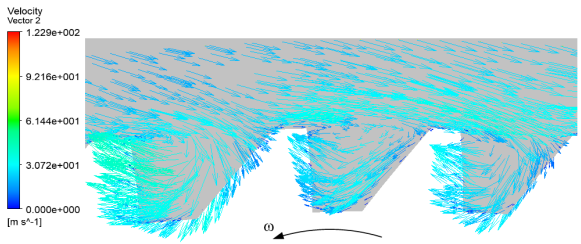

Fig. 11. *Velocity vector diagram of fluid around gear* [5]

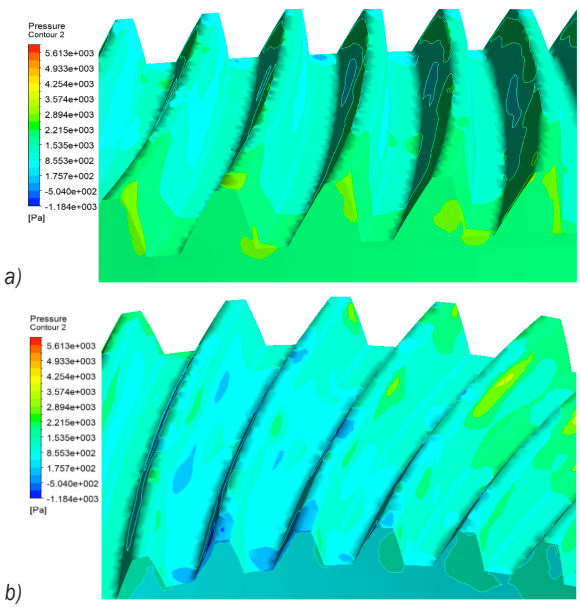

Fig. 12. *Pressure distribution in tooth space; a) pressure surface, and b) suction surface* [5]

Under the condition of high speed and heavy load, the aviation spiral bevel gear is lubricated by oil injection. The two gears respectively accelerate the fluid around their teeth and carry some fluid to collide and squeeze at their engagement, thus consuming the power of the gear system. Through CFD-POST, it can be calculated that the windage moment on a certain surface of the gear is the vector sum of the pressure and viscous force on all elements of the surface to the specified axis. The calculation equation, Eq. (7) is:

$$\mathbf{M}=\sum_{i=1}^{n}\left(\mathbf{r}\times\mathbf{F}_{p}\right)+\sum_{i=1}^{n}\left(\mathbf{r}\times\mathbf{F}_{\upsilon}\right), \tag{7}$$

where $\mathbf{M}$ is the calculated windage torque; $\mathbf{F}_p$ and $\mathbf{F}_\upsilon$ are the pressure and viscous force vector on the element surface, respectively; $\mathbf{r}$ the setting axis vector; n is the number of elements on the selected wall.

Then the windage power loss of the spiral bevel gear pair is:

$$P_{\mathrm{w}}=\sum_{i=1}^{2}M_i\omega_i, \tag{8}$$

where M is the total windage torque value of gear; ω is the angular speed of gear; i takes 1 or 2 to indicate the pinion or gear.

3 RESULTS AND DISCUSSION

3.1 Dimensionless Analysis of Windage Moment

From the above analysis, it can be seen that the windage power loss of the gear with oil injection lubrication is not only related to the geometric parameters and working condition of the gear but also to the fluid characteristics, such as density and viscosity. Therefore, in order to concentrate the influence of these parameters on windage torque and enhance the comparability of calculation results, all results are dimensionless. The dimensionless coefficient C_M of windage torque is obtained with the following equation (Eq. (9)):

$$C_M=\frac{M}{1/2\,\rho\omega^2R^5}, \tag{9}$$

where M is windage torque; ω is the gear angular velocity; R is the pitch radius of the gear; ρ is the equivalent density of oil-gas two-phase flow.

Fig. 13 shows the relationship between the dimensionless moment coefficient and the rotational Reynolds number, showing the windage torque obtained by test and numerical simulation. The rotational Reynolds number is:

$$Re=\frac{\rho_e\omega R^2}{\mu_e}, \tag{10}$$

It can be seen from Fig. 13 that the CFD numerical value is in good qualitative agreement with the experimental measurement data; however, from the quantitative perspective, the numerical

result is always lower than the experimental value. The best consistency between the two is in the range of Re = 2.0×10^5~3.0×10^5, where the corresponding gear shaft speed is 5500 rpm to 7500 rpm, and the percentage difference of torque value is less than 10 %. The largest difference is at 2500 rpm, when the corresponding Reynolds number is about 0.7×10^5, and the percentage difference is as high as 37 %. This is mainly because there are some uncertainties in the experiment, which are dominant in the lower rotation speed. It can also be found from Fig. 13 that the shape of C_M curves of the experiment and simulation is similar, all test points change near a curve, and the C_M value decreases slowly with the increase of Re, when the data with the highest uncertainty at the speed of 2000 rpm to 3000 rpm can be ignored. This is consistent with the experimental results of Massini et al. [21], Rapley et al. [27] and Johnson et al. [29].

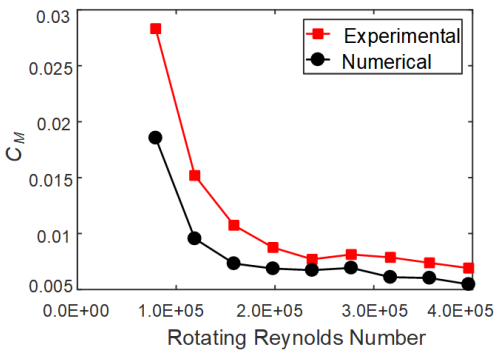

Fig. 13. *Graph of Cm against Rotating Reynolds Number*

3.2 Mechanical Characteristics of Windage Power Loss

When the gear rotates at a high speed in the oil-gas two-phase flow, in addition to the pressure action of the fluid on the gear surface, due to the viscosity of the fluid, the fluid will produce viscous resistance on each surface of the gear in contact with it, which also constitutes a small part of the windage losses of gears. The distribution of pressure and viscous force of gear pair is shown in Fig. 14.

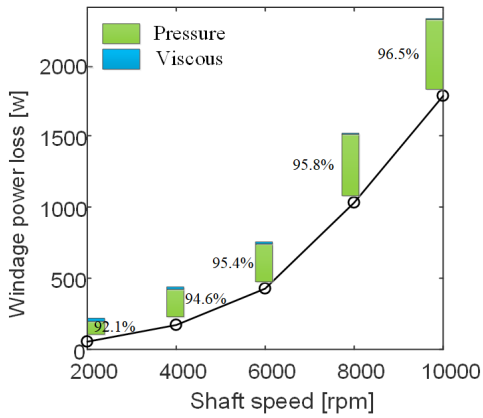

Fig. 15. *Gear windage power loss of numerical investigation against rotating speed*

It can be seen from Fig. 14 that there is a maximum pressure value on the into-meshing side, while the minimum pressure appears on the tooth surface and end face near the gear out-of-meshing side, and the pressure value is less than the standard atmospheric pressure, which is negative pressure. Since the spiral bevel gear is point meshing, one possible reason is that the volume between the meshing teeth shrinks

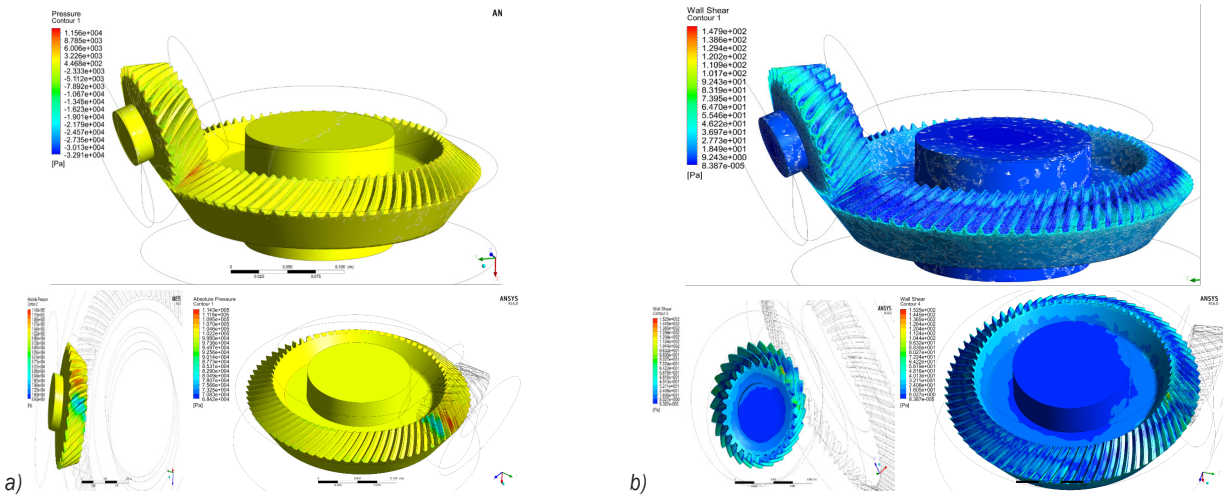

Fig. 14. *The distribution of pressure and viscous force on the gears; a) pressure nephogram, and b) viscous pressure nephogram*

and the fluid is squeezed during the meshing process, resulting in high pressure here. While the gear teeth on the out-of-meshing side exit from the meshing state and separate rapidly, the two-phase flow around them has been squeezed out or thrown out. Also, the space between the gear teeth increases rapidly, so that the pressure on the out-of-meshing side decreases or even becomes negative pressure. The principle of this phenomenon is similar to that of gear pump.

Fig. 15 shows the variation curve of windage power loss caused by pressure difference force and viscous force with speed. According to the mechanism of windage loss, it can be seen that the pressure difference torque and viscous torque acts on the tooth surface together, while the end face, cone surface and circumferential surface only have viscous torque. At the same time, it can be observed from Fig. 15 that the windage loss caused by pressure difference force accounts for more than 90 % of it. Therefore, from the analysis of mechanical mechanism, the windage power loss of gears is mainly determined by fluid inertia. The bar chart in the figure also shows that the percentage of power loss caused by differential pressure torque in the total windage loss increases with the increase of speed, that is, the higher the gear speed, the more significant the pressure effect.

3.3 Energy Characteristics of Windage Power Loss

The above research shows that the windage power loss of the gear is the kinetic energy loss of the gear caused by the windage torque (differential pressure force and viscous force) when the gear rotates at high speed. When the gearbox is sealed, the lost kinetic energy is divided into two parts, that is, one part is converted into heat energy by the friction between the fluid and the gear surface, and the other part is converted into fluid kinetic energy. The distribution of lubricating oil inside the gearbox and on the gear surface at different time is shown in Fig. 16.

As shown in Fig. 16, due to the revolution speed of pinion is greater than that of gear, the rotation angle of pinion is larger at the same time, so more lubricating oil is carried by the pinion at the beginning of simulation. After a period of time, the lubricating oil carried by the two gears converges and collides near the meshing point, and most of the lubricating oil on the tooth surface is thrown off and falls on the wall of the gearbox.

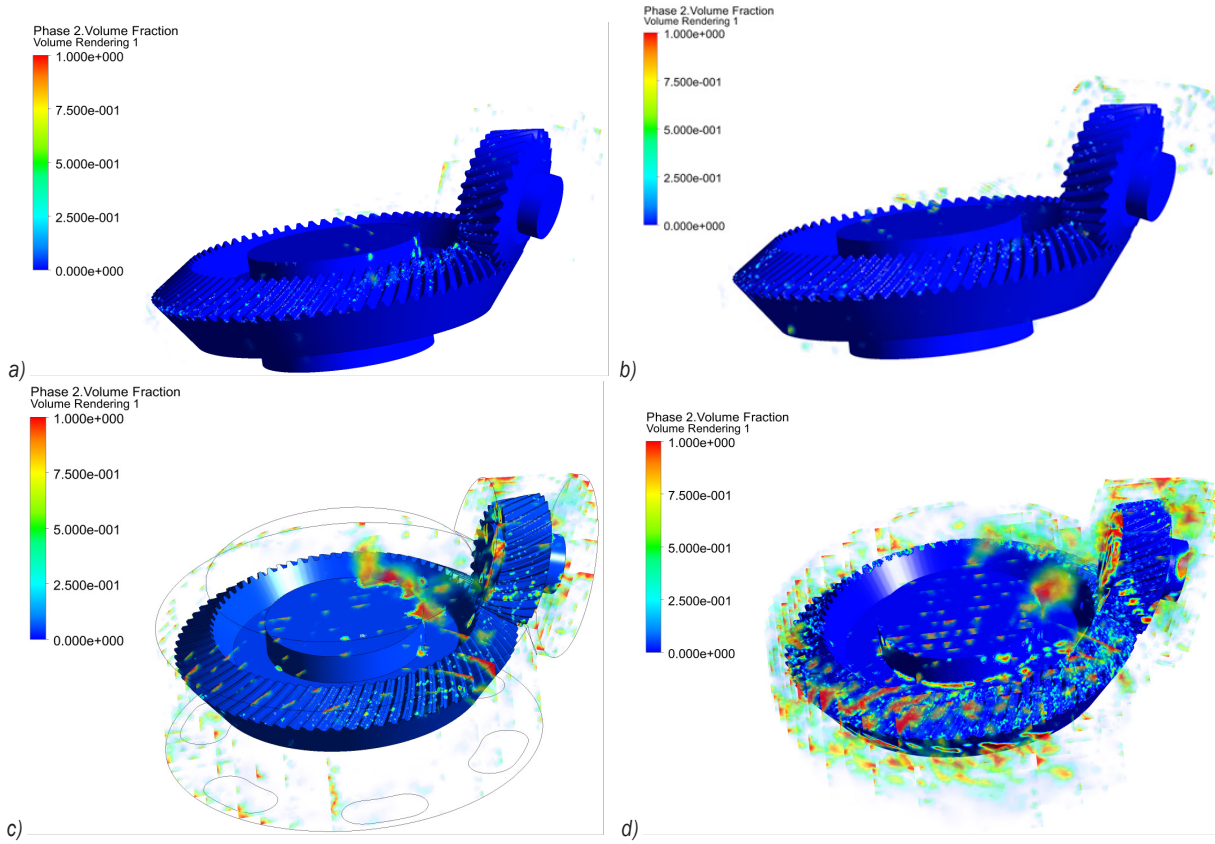

Fig. 16. *Lubricating oil distribution of gearbox at: a) t = 0.005 s, b)) t = 0.010 s, c)) t = 0.015 s, and d)) t = 0.021 s*

Table 7 shows the turbulent kinetic energy and turbulent dissipation rate at different oil-jet velocities obtained by mass-weighted integration of the entire computational fluid domain using CFD post-processing.

Table 7. *Turbulent kinetic energy and dissipation rate with different oil-jet velocities*

Oil-jet velocity [m/s]	Turbulent kinetic energy [kg·m²/s²]	Turbulent dissipation rate [kg·m²/s³]
10	0.049	335.32
20	0.067	366.25
30	0.091	554.46
40	0.122	725.61
50	0.131	836.57

The turbulent kinetic energy represents the intensity of the turbulent motion inside the gear box. The turbulent dissipation rate represents the amount of fluid kinetic energy lost due to the turbulent motion of the oil-air mixture. As can be seen from Table 7, turbulent kinetic energy and the turbulent dissipation rate both increase with the increase of oil jet velocity. This indicates that the turbulent motion of oil and gas mixture in computational fluid domain becomes increasingly intense. Also, a greater amount of energy is consumed by fluid movement, resulting in the increasing of windage power loss of the gear pair. The relationship between the windage moment and the injection pressure obtained by the orthogonal experimental fitting formula, Eq. (2) in Section 2.4, shows that the results in Table 7 are consistent with the experimental conclusions.

4 CONCLUSIONS

1. A method for measuring the windage losses of spiral bevel gears with oil injection lubrication is proposed by establishing an open power flow windage loss experimental rig. According to the torque values measured with experiments under different working conditions, the corresponding windage torque and rig driveline torque values of the system are calculated.
2. The interaction effect of different oil injection lubrication parameters on windage power loss is studied by orthogonal experiment. According to the experimental data, the formula for calculating the windage power loss of gear pair under oil injection lubrication is obtained. The results show that the shaft speed has the greatest influence on the windage power loss of the gear pair. The second is the injection pressure, adjusting the injection pressure to change the injection quantity, thereby affecting the volume fraction of lubricating oil around the gear. The injection temperature has the least influence.
3. The CFD numerical model of the spiral bevel gear based on dynamic mesh is established. The fluid distribution, velocity field, and pressure field around the gear are analysed, and the mechanical and energy characteristics of windage power loss are obtained.
4. The dimensionless processing of the experimental data and simulation values of the windage torque of spiral bevel gears is carried out, and the variation law of the dimensionless windage torque coefficient with the rotational Reynolds number is obtained. The results show that the CFD values are in good agreement with the experimental data. With the increase of rotational Reynolds number, the dimensionless windage moment coefficient changes little and fluctuates on an almost horizontal line.

5 REFERENCES

[1] Dai, Y., Ma, F., Zhu, X., Su, Q., Hu, X. (2019). Evaluation and optimization of the oil jet lubrication performance for orthogonal face gear drive: Modelling, simulation and experimental validation. *Energie*s, vol. 12, no. 10, p. 1935-1947, **DOI:10.3390/en12101935**.

[2] Fondelli, T., Andreini, A., Facchini, B. (2018). Numerical investigation on windage losses of high-speed gears in enclosed configuration. *AIAA Journal*, vol. 56, no. 5, p. 1910-1921, **DOI:10.2514/1.J055871**.

[3] Dong, C., Pei, W., Ren, Z. (2022). Experimental Research on Transmission Characteristics of Elliptic Gear Transmission Systems. *Strojniški vestnik - Journal of Mechanical Engineering*, vol. 68, no. 11, p. 702-712, **DOI:10.5545/sv-jme.2022.332**.

[4] Concli, F., Gorla, C. (2017). Numerical modeling of the churning power losses in planetary gearboxes: An innovative partitioning-based meshing methodology for the application of a computational effort reduction strategy to complex gearbox configurations. *Lubrication Science*, vol. 29, no. 7, p. 455-474, **DOI:10.1002/ls.1380**.

[5] Li, L., Wang, S., Zou, H., Cao, P. (2022). Windage Loss Characteristics of Aviation Spiral Bevel Gear and Windage Reduction Mechanism of Shroud. *Machine*s, vol. 10, no. 5, art. ID 390, **DOI:10.3390/machines10050390**.

[6] Dong, C., Liu, Y., Zhao, G. (2021). A Method for Calculating Elliptic Gear Transmission Efficiency Based on Transmission Experiment. *Strojniški vestnik - Journal of Mechanical Engineering*, vol. 67, no. 11, p. 557-569, **DOI:10.5545/sv-jme.2021.7318**.

[7] Handschuh, R., Kilmain, C., Ehinger, R., Sinusas, E. (2013). Gear design effects on the performance of high speed helical

gear trains as used in aerospace drive systems. *AHS Annual Forum and Technology Display*, No. E-18652-1, p. 668-677.

[8] Kumar, V., Kumar, A., Yadav, SK., Yadav, A., Prasad, L., Winczek, J. (2022). Numerical Analysis on a Constant Rate of Kinetic Energy Change Based a Two-Stage Ejector-Diffuser System. *Strojniški vestnik - Journal of Mechanical Engineering*, vol. 68, no. 5, p. 368-373, **DOI:10.5545/sv-jme.2011.7538**.

[9] Li, L., Wang, S., Zhang, X., Li, Z., Li, F., Zou, H. (2022). Numerical calculation analysis and characteristic research on windage loss of oil-jet lubricated aviation gear pair. *International Journal of Aerospace Engineering*, vol. 6, no. 12, p. 1687-1699, **DOI:10.1155/2022/7499587**.

[10] Ding, H., Li, H., Shao, W., Tang, J. (2021). Prediction and control for local bearing contact-based collaborative grinding of non-orthogonal aerospace spiral bevel gears. *Mechanical Systems and Signal Processing*, vol. 160, art. ID 107841. **DOI:10.1016/j.ymssp.2021.107841**.

[11] Li, S., Li, L. (2021). Computational investigation of baffle influence on windage loss in helical geared transmissions. *Tribology International*, vol. 156, art. ID 106852, **DOI:10.1016/j.triboint.2020.106852**.

[12] Okorn, I., Nagode, M., Klemenc, J. (2021). Operating Performance of External Non-Involute Spur and Helical Gears: A Review. *Strojniški vestnik - Journal of Mechanical Engineering*, vol. 67, no. 5, p. 256-271, **DOI:10.5545/sv-jme.2020.7094**.

[13] Anderson, N., Loewenthal, S. (1981). Effect of geometry and operating conditions on spur gear system power loss. *Journal of Mechanical Design*, vol. 103, no. 1, p. 151-159, **DOI:10.1115/1.3254854**.

[14] Dawson, P.H. (1984). Windage loss in larger high-speed gears. *Proceedings of the Institution of Mechanical Engineers, Part A: Power and Process Engineering*, vol. 198, no. 1, p. 51-59, **DOI:10.1243/PIME_PROC_1984_198_007_02**.

[15] Diab, Y., Ville, F., Velex, P. (2006). Investigations on power losses in high-speed gears. *Proceedings of the Institution of Mechanical Engineers, Part J: Journal of Engineering Tribology*, vol. 220, no. 3, p. 191-198, **DOI:10.1243/13506501JET1**.

[16] Winfree, D.D. (2000). Reducing gear windage losses from high speed gears. *International Design Engineering Technical Conferences and Computers and Information in Engineering Conference*, p. 747-756, **DOI:10.1115/DETC2000/PTG-14449**.

[17] Seetharaman, S., Kahraman, A. (2009). Load-independent spin power losses of a spur gear pair: model formulation. *Journal of Tribology*, vol. 131, no. 2, p. 181-193, **DOI:10.1115/1.3085943**.

[18] Ruzek, M., Ville, F., Velex, P., Boni, J.B., Marchesse, Y. (2019). On windage losses in high-speed pinion-gear pairs. *Mechanism and Machine Theory*, vol. 132, no. 5, p. 123-132, **DOI:10.1016/j.mechmachtheory.2018.10.018**.

[19] Delgado, I.R., Hurrell, M.J. (2017). Experimental investigation of shrouding on meshed spur gear windage power loss. *73rd Annual Forum and Technology Display*, NASA/TM-2017-219536.

[20] Handschuh, R. F., Hurrel, M.J. (2010). Initial experiments of high-speed drive system windage losses. *International Conference on Gears*, art. ID 20100036224.

[21] Massini, D., Fondelli, T., Andreini, A., Facchini, B., Tarchi, L., Leonardi, F. (2018). Experimental and numerical investigation on windage power losses in high speed gears. *Journal of Engineering for Gas Turbines and Power*, vol. 140, no. 8, **DOI:10.1115/GT2017-64948**.

[22] Maccioni, L., Chernoray, V.G., Mastrone, M.N., Bohnert, C., Concli, F. (2022). Study of the impact of aeration on the lubricant behavior in a tapered roller bearing: Innovative numerical modelling and validation via particle image velocimetry. *Tribology International*, vol. 165, art. ID 107301, **DOI:10.1016/j.triboint.2021.107301**.

[23] Mastrone, M.N., Concli, F. (2021). CFD simulations of gearboxes: implementation of a mesh clustering algorithm for efficient simulations of complex system's architectures. *International Journal of Mechanical and Materials Engineering*, vol. 16, no. 1, art. no. 12, **DOI:10.1186/s40712-021-00134-6**.

[24] Gorla, C., Concli, F., Stahl, K., Höhn, B.R., Michaelis, K., Schultheiß, H., Stemplinger, J.P. (2013). Hydraulic losses of a gearbox: CFD analysis and experiments. *Tribology International*, vol. 66, p. 337-344, **DOI:10.1016/j.triboint.2013.06.005**.

[25] Fondelli, T., Andreini, A., Da Soghe, R., Facchini, B., Cipolla, L. (2015). Numerical simulation of oil jet lubrication for high speed gears. *International Journal of Aerospace Engineering*, vol. 2015, art. ID 752457, **DOI:10.1155/2015/752457**.

[26] Farrall, M., Simmons, K., Hibberd, S., Young, C. (2005). Computational investigation of the airflow through a shrouded bevel gear. *ASME Turbo Expo 2005: Power for Land, Sea, and Air*, no. 3, p. 1259-1265, **DOI:10.1115/GT2005-68879**.

[27] Rapley, S., Eastwick, C., Simmons, K. (2008). Effect of variations in shroud geometry on single phase flow over a shrouded single spiral gear. *Heat Transfer, Parts A and B*, vol. 4, **DOI:10.1115/gt2008-50633**.

[28] Webb, T.A., Eastwick, C., Morvan, H. (2010). Parametric modelling of a spiral bevel gear using CFD. P*roceedings of the ASME Turbo Expo*, p. 229-238, DOI:10.1115/GT2010-22632.

[29] Johnson, G., Chandra, B., Foord C., Simmons, K. (2009). Windage power losses from spiral bevel gears with varying oil flows and shroud configurations. *ASME Turbo Expo: Power for Land, Sea, & Air*, vol. 131, no. 4, art. ID 041019, **DOI:10.1115/1.3072519**.

[30] Simmons, K., Johnson, G., Wiedemann, N. (2012). Effect of pressure and oil mist on windage power loss of a shrouded spiral bevel gear. *Journal for Engineering for Gas Turbines and Power*, vol. 134, no. 8, art. ID 081202, **DOI:10.1115/1.4005984**.

[31] Harris, T.A. (1984). Rolling Bearing Analysis, 2nd ed., Wiley, New York.

[32] Liang, R. (2008). Orthogonal test design for optimization of the extraction of polysaccharides from Phascolosoma esulenta and evaluation of its immunity activity. *Carbohydrate Polymers*, vol. 73, no. 4, p. 558-563, **DOI:10.1016/j.carbpol.2007.12.026**.

[33] AGMA, (1995). *Fundamental Rating Factors and Calculation Methods for Involute Spur and Helical Gear (Metric Version),* American Gear Manufacturers Association, 2101-C95.